

1 How are oxygen budgets influenced by dissolved iron and 2 growth of oxygenic phototrophs in an iron-rich spring system? 3 Initial results from the Espan Spring in Fürth, Germany

4 Inga Köhler¹, Raul E. Martinez², David Piatka¹, Achim J. Herrmann³, Arianna Gallo³, Michelle
5 M. Gehringer³, Johannes A.C. Barth¹

6 ¹Department of Geography and Geosciences, GeoZentrum Nordbayern, Schlossgarten 5, Friedrich-Alexander-
7 Universität FAU, Erlangen, 91054, Germany

8 ²Max-Planck-Institute for Biogeochemistry, Jena, 07745, Germany

9 ³Division of Microbiology, Technische Universität, Kaiserslautern, 67663 Germany

10 Correspondence to: Inga Köhler (inga_koehler@gmx.de)

11 **Abstract.** At present most knowledge on the impact of iron on ¹⁸O/¹⁶O ratios (i.e. $\delta^{18}\text{O}$) of dissolved oxygen (DO)
12 under circum-neutral conditions stems from experiments carried out under controlled laboratory conditions. These
13 showed that iron oxidation leads to an increase in $\delta^{18}\text{O}_{\text{DO}}$ values. Here we present the first study on effects of
14 elevated Fe(II) concentrations on the $\delta^{18}\text{O}_{\text{DO}}$ in a natural, iron-rich circum-neutral watercourse. Our results show
15 that iron oxidation was the major factor ~~dominating the~~ ~~to cause rising~~ oxygen isotopic ~~signatures~~ in the first 85
16 meters of the system in the cold season (~~December~~-February) and for the first 15 meters during the warm season
17 (May). ~~This trend existed despite a constant oxygen supply from the atmosphere.~~ Further along the course of ~~the~~
18 ~~spring stream and associated small stream system~~, the $\delta^{18}\text{O}_{\text{DO}}$ decreased towards values known for atmospheric
19 equilibration ~~at 24.6 ‰ during both seasons.~~ ~~This Possible drivers for this decrease~~ may be ~~due to~~ reduced iron
20 oxidation, increased atmospheric exchange and ~~photosynthetic~~ DO production ~~by oxygenic phototrophic algae~~
21 ~~mats.~~ The presence of oxygenic phototrophic mats suggested their involvement in the observed decrease in $\delta^{18}\text{O}_{\text{DO}}$
22 ~~values.~~ In the cold season, the $\delta^{18}\text{O}_{\text{DO}}$ values stabilized around atmospheric equilibrium ~~at +24.6 ‰~~, whereas in
23 the warm season ~~stronger influences by oxygenic photosynthesis caused values down values decreased to +21.8~~
24 ~~‰.~~ ~~This suggests stronger influences by oxygenic photosynthesis.~~ ~~In the warm season after About~~ 145 meters
25 downstream of the spring, the $\delta^{18}\text{O}_{\text{DO}}$ increased again ~~in the warm season~~ until it reached ~~the~~ atmospheric
26 equilibrium ~~value of +24.6 ‰.~~ This trend can be explained by a respiratory consumption of DO combined with a
27 ~~relative~~ decrease in photosynthetic activity ~~and increasing atmospheric influences.~~ Our study shows that dissolved
28 Fe(II) can exert strong effects on the $\delta^{18}\text{O}_{\text{DO}}$ of a natural circum-neutral spring system even ~~though under a~~ constant
29 supply of atmospheric ~~O₂ oxygen occurs.~~ ~~However, In in~~ the presence of active photosynthesis, with active supply
30 of ~~oxygen—O₂~~ to the system, direct effects of Fe oxidation on the $\delta^{18}\text{O}_{\text{DO}}$ value becomes masked.
31 ~~However~~ Nonetheless, critical Fe(II) concentrations may indirectly control DO budgets by enhancing
32 photosynthesis, particularly if cyanobacteria are involved.

33 1 Introduction

34 Oxygen is the most abundant (45.2 %) and iron the fourth most abundant (5.8 %) element on earth (Skinner, 1979).
35 Such huge global reservoirs render these elements critically important in global biogeochemical cycles. In addition,
36 their reactivity is exceptional: O₂ is a powerful oxidation agent while Fe can cover oxidation states from -4 to +7
37 in extreme cases, with the most commonly known ones being 0, +2 and +3 (Lu et al., 2016).

38 Iron is also an essential trace element in many biological processes, including photosynthesis, oxygen transport
39 and DNA biosynthesis (Kappler et al., 2021). This closely links to the formation and dissolution of Fe oxides.
40 ~~These common forms of metal oxides~~ ~~that~~ may enhance or reduce availabilities of both elements in the water
41 column and pore waters and thus may largely regulate aqueous life.

hat formatiert: Deutsch (Deutschland)

hat formatiert: Tiefgestellt

hat formatiert: Tiefgestellt

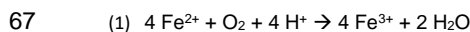
42 In aqueous environments, dissolved oxygen (DO) is one of the most essential ecosystem parameters and, despite
43 its moderate solubility (e.g. 9.3 mg/L⁻¹ at 20 °C), it assumes a central role in respiration, primary production and
44 Fe-oxidation (Pusch, 1996). The concentration of DO coupled to its stable isotope ¹⁸O/¹⁶O ratios (i.e. δ¹⁸O) can
45 yield additional information about sources and sinks, including atmospheric input, photosynthesis, respiration and
46 mineral oxidation.

47 When equilibrated with the atmosphere, δ¹⁸O_{DO} values typically range around a value of + 24.6 ‰ (Mader et al.,
48 2017) while photosynthesis and respiration can change these isotope ratios (Guy et al., 1993; Kroopnick, 1975).
49 The splitting of water molecules during photosynthesis hardly produces an isotope discrimination and the resulting
50 DO ~~should has-have~~ the same isotope value as the surrounding water (Guy et. al., 1993; Eisenstadt et al., 2010).
51 Meteoric water in temperate climates is normally depleted in ¹⁸O and therefore the photosynthetic oxygen in these
52 areas varies between - 10 to - 5 ‰ (Quay et. al., 1995; Wang and Veizer, 2000). Respiration, on the other hand,
53 preferentially accumulates ¹⁶O and enriches the remaining DO in ¹⁸O ~~and~~. This process yields δ¹⁸O_{DO} values
54 between + 24.6 and + 40 ‰ (Guy et. al., 1993).

55 Additionally, oxidation of metals such as Fe also lead to a rise/increases in δ¹⁸O_{DO} (Lloyd, 1968; Taylor and
56 Wheeler, 1984; Wassenaar and Hendry, 2007; Oba and Poulsen, 2009 a,b; Pati, 2016). Mostly, the impacts of Fe
57 oxidation on δ¹⁸O_{DO} values have been investigated experimentally under controlled conditions (Oba and Poulsen,
58 2009b; Pati et al., 2016). ~~However~~ As a new aspect, ~~so far~~ these dynamics were not studied in open water systems
59 such as springs and rivers so far. New field investigations might reconcile Variations-variations in the fractionation
60 factors obtained in the abovementioned studies. At current ~~resulted from~~ they are thought to result from differences
61 in temperature, pH and initial Fe(II) concentrations that could be outlined under abiotic conditions.

62 Dissolved Fe(II) in natural systems may have primary and secondary impacts on DO concentration and its δ¹⁸O_{DO}
63 values. The primary influence originates from the O₂ binding by iron oxidation (equation 1). This leads to decreases
64 of the DO and causes simultaneous increases of ~~the~~ δ¹⁸O_{DO} values (Wassenaar and Hendry, 2007; Smith et al.,
65 2011; Parker et al., 2012 and Gammons et al., 2014).

66



68

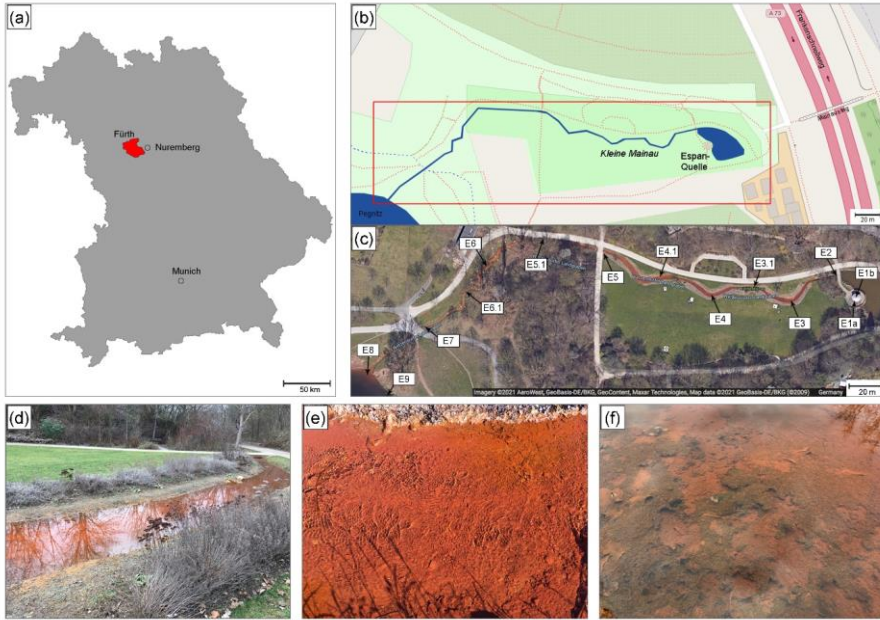
69 Dissolved Fe(II) can also have secondary (i.e. indirect) influences on the DO content and the δ¹⁸O_{DO}. This happens
70 when it acts as an essential micronutrient to cause growth-stimulating effects on O₂-producing and respiring
71 microorganisms. These influences of Fe(II) on DO and δ¹⁸O_{DO} in circum-neutral aquatic systems have so far
72 received little attention because of the following reasons:

- 73 (1) Fe oxidation often masks δ¹⁸O_{DO} values created by respiration, photosynthetic and atmospheric oxygen
74 and
75 (2) adequate Fe(II)-rich circum-neutral model systems are scarce on modern earth. This is due to the high reactivity
76 of iron with DO.

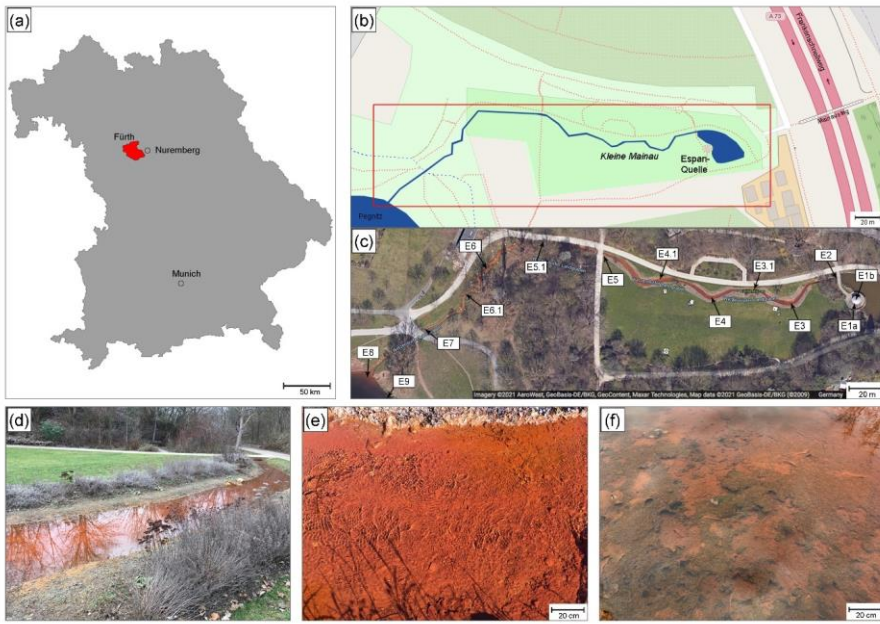
77

78 To the best of our knowledge, no study so far has systematically investigated the influences of elevated Fe(II)
79 concentrations on δ¹⁸O_{DO} values in a natural and circum-neutral iron-rich system. In order to bridge this gap, we
80 investigated the aqueous chemistry and δ¹⁸O_{DO} values in the iron-rich Espan Spring in Fürth, Germany (Fig. -1).
81 This Fe(II)-rich artesian spring offers a complex biogeochemical natural field site to analyse effects of different
82 Fe(II) contents on the DO and δ¹⁸O_{DO} values.

Formatiert: Block, Abstand Nach: 0 Pt.



83



84

85 **Figure 1** Overview ~~over~~ of the Espan Spring in Fürth, Germany. a) and b): Location of the spring in Bavaria and
 86 the city of Fürth. c) Satellite image (~~Google maps~~) of the spring ~~by Google maps~~ showing the distinct red colour.
 87 d) to f) Detailed photos of the system. ~~Image~~ d) displays the stream between sampling points E4 and E5, ~~image is~~

e) shows sampling point E3 (with the bank of the ~~WL~~ water line in the upper part of the picture) and ~~image f)~~ displays sampling point E4.1 with algae and cyanobacteria mats.

The aims of this study were to establish an inventory of biology together with Fe and oxygen budgets in this ~~exceptional~~ natural spring and stream system. We further aimed to investigate how increased Fe(II)-levels influence the oxygen budget of the system and whether a combination of DO and $\delta^{18}\text{O}_{\text{DO}}$ measurements can help to ~~assess asses~~ this effect. This is also timely because environmental impacts of Fe(II) ~~are become~~ increasingly ~~being~~ recognised as ~~having~~ for their negative effects on ecosystems such as ~~in~~with the browning or brownification phenomenon (Kritzberg and Ekström, 2011; Weyhenmeyer et al., 2014; Kritzberg et al., 2020). During this process, increased iron levels can consume oxygen, cause algae blooms and reduce water ~~potability~~quality and thus ~~may~~ affect aqueous ecosystems and their services. This is also timely because environmental impacts of Fe(II) are increasingly being recognised as problematic. This is for instance the case with phenomena of browning or brownification (Kritzberg and Ekström, 2011; Weyhenmeyer et al., 2014; Kritzberg et al., 2020). During this process, increased iron levels can consume oxygen, cause algae blooms and reduce water potability and thus affect aqueous ecosystems and their services. Here we describe a first complete spatial sampling campaign in the cold and warm season with Fe(II), Fe(III), DO and its stable $^{18}\text{O}/^{16}\text{O}$ isotope ratios ~~as well~~together with ~~as~~ field parameters (pH, T, DO, ~~pe~~, electrical conductivity). ~~from a cold season and warm season campaign.~~ This study contributes to the knowledge of Fe oxidation in natural systems and delivers implications of hardly explored seasonal dynamics in Fe(II) rich systems.

hat formatiert: Schriftart: (Standard) Times New Roman, 10 Pt.

2 Methods

2.1 Study site

The Espan Spring is located in the city of Fürth, Germany (49°28'15.8"N 11°00'53.0"E, Fig. 1). It is an artesian spring that originates from a confined aquifer that was tapped by a drilling project in 1935 from a depth of 448.5 m below ground. The water originates from the so called "lower mineral water horizon", ~~which~~This horizon is dominated by artesian inflow from the lower Buntsandstein Formation. The Buntsandstein in Fürth consists of red sandstone layers ~~which~~that are composed of light reddish to yellowish-white-grey sandstones of different grain sizes. ~~Intere~~related with ~~the~~ sandstones are intercalated with differentvarious rubble, conglomerate, and clay layers as well as thin gypsum and salt ~~layers~~(Birzer, 1936). Three noticeable conglomerate layers are ~~interposed~~present in the sequence of Buntsandstein layers. Birzer (1936) distinguished the Upper Buntsandstein from the Upper Main Buntsandstein by the Main Conglomerate which can be found at a depth of 321 to 324 m. The Middle Boulder Layer at a depth of 370 to 371 m separates the Upper from the Lower Main Buntsandstein and the so-called Eck'sche Conglomerate at a depth of 433 to 440 m which separates the Lower Main Buntsandstein from the Lower Buntsandstein (Birzer, 1936).

At a depth of 370 to 439 m, mineral water flows into the borehole from the Upper and Lower Main Bunter Sandstone and from the Eck conglomerate. This water, which is caught in the red sandstone and has a temperature of about +22°C, was called the "Lower Mineral Water Horizon"; in 1936 its yield was about 10 ~~L/s~~ s⁻¹ at a water temperature of +23°C (Kühnau 1938). The water of this lower spring horizon is under highartesian pressure, ~~so~~

hat formatiert: Hochgestellt

125 ~~and that it flows out at the earth's surface~~exits the spring with a head of 13 m above ground level (Birzer, 1936).
126 ~~Nowadays the Espan Spring has a~~and causes the constant yield of the Espan Spring of about 5 L s⁻¹/s even today.

hat formatiert: Hochgestellt

127 After the water exits the ~~well basin~~ in a pavilion with a temperature of ~ 20 °C, it discharges into a stream of about
128 300 m length that is known as the "Wetzendorfer Landgraben (WL)". ~~This small stream that~~ drains into the Pegnitz
129 River without any further tributaries (Fig. 1b, c). The water can be classified as a Na-Ca-Cl-SO₄ mineral water
130 with initially undersaturated DO values of 2.3 mg/L and Fe(II) contents of up to 6.6 mg/L (Table 1). Figure 1c
131 shows an aerial image of the spring and stream system that shows a distinct red coloring of the stream bed. The
132 most plausible explanation ~~for this is that this~~ coloring originates from ~~are~~ iron-oxide-precipitates (Fig. 1d, e). ~~The~~
133 ~~WL has a water depth between 8-10 cm and shows little fluctuations.~~

134 2.2 Sampling procedures

135 Two field campaigns were performed in February and May 2020, during which water was collected at 14 locations
136 along the stream ~~between 8 am and 12 pm. The water was collected at about 10 cm depth below the surface.~~ The
137 onsite parameters pH (±0.05; instrument precision), temperature (±0.1 °C), electrical conductivity, Eh and DO (all
138 ±2 %) were measured with a HACH HQ 40d multi parameter instrument. Alkalinity titrations were carried out
139 with a Hach Titrator with a bromocresol-green indicator. Fe(II) and Fe(III) contents were measured using an iron
140 (II/III) cuvette test set by Hach in combination with a portable Hach spectrophotometer (model DR 2800).

141 Samples for ¹⁸O/¹⁶O ratios of DO were collected in 12-mL Exetainers® (Labco Ltd. Lampeter, U.K.) that were
142 prepared with 10 µL of a saturated HgCl₂ solution to prevent secondary biological activity after sampling
143 (Wassenaar and Koehler, 1999; Parker et al., 2005 and 2010). The Exetainers were filled with syringe-filtered
144 water via 0.45 µm pore size nylon filters until they were entirely full and free of air bubbles. They were then
145 carefully closed with screw caps with a butyl septum in order to avoid atmospheric contamination. Test series
146 showed that the amount of atmospheric contamination during this filling procedure is usually negligible (Mader et
147 al. 2018).

148 Samples for water isotopes were collected in 15 mL Falcon tubes ~~bottles~~ and treated in the same manner as the
149 ones for DO isotope measurements, except for preservation with HgCl₂. ~~Instead, the All~~ samples were stored in a
150 mobile refrigerator box at 4 °C directly after collection and carried to the laboratory where they were measured
151 within 24 h.

152 2.3 Identification of possible mineral precipitates

153 In order to determine possible mineral precipitate data for the pH, pe ~~(expresses the activity~~activity~~the negative~~
154 ~~decadic activity of e~~available -electrons in factors of 10), temperature, alkalinity (as CaCO₃), as well as cations
155 and anions, the specific sampling points were fed into the program PhreeqC (Version 3; Parkhurst and Appelo,
156 2013) for calculation of saturation indices. The database used ~~for these calculations~~ was Wateq4.

Formatiert: Standard

hat formatiert: Englisch (Vereinigte Staaten)

157 2.5 Laboratory methods

158 2.5.1 Identification of cyanobacteria

159 Samples were collected in a preliminary field assessment at the anoxic piping where the spring flows into the creek
160 (E2), in the middle of the creek at ~~the~~ first small pond after the water had contact to the atmosphere (E3) and about

161 5 m downstream of this pond from an algal mat with bubbles on the surface (E4). Samples for cyanobacterial
162 isolation were collected in sterile 2-mL Sarsted tubes and sealed. Samples for microscopic analysis were
163 collected with a 75 % ethanol sterilised spatula and placed in a sterile 6 cm petri dish (Sarsted, Germany).
164 Immediately after returning from the sampling site, samples were embedded in 1.5 % Agarose in de-ionized water
165 to preserve the structure of the bio mats during further handling and shipping.
166 Microscopic analysis was performed on thin sections of the embedded mats using a CLSM-type microscope (LSM
167 880, Carl Zeiss), using modified acquisition settings from Jung *et al.* (2019) to discriminate between cyanobacterial
168 (chlorophyll-*a* (chl-*a*) and phycobiliproteins (PBP)) and green algal (chl *a*) fluorescence. Laser
169 transmission images were also generated using the 543 nm laser.

hat formatiert: Schriftart: (Standard) Times New Roman, 10 Pt.

170 A spatula tip of green coloured mat was used to inoculate 5 mL of BG11 medium (Stanier *et al.*, 1971) in a well
171 of a 6-well plate and incubated for 3 weeks at 24 °C on a 16:8 day:night cycle with illumination at 15 μmols
172 photons m⁻²m⁻²/s⁻¹ under an OSRAM L30W/840 LUMINLUX Cool White bulbs. Individual Cyanobacterial species
173 were picked from the mat cultures under a Nikon SMZ-U Zoom binocular microscope for further subculturing on
174 1 % agar solidified BG11 plates, as well as liquid culture. Isolates were observed under an Olympus BX53 light
175 microscope and their morphologies recorded using an Olympus DP26 Camera. The number of cells per filament
176 and cell dimensions were measured using ImageJ 1.47v software. DNA was extracted (Gehring *et al.*, 2010)
177 from one axenic isolate of a microscopically identified *Persinema* species of cyanobacteria. The 16S rDNA gene
178 and intergenic spacer sequence was amplified by the SSU-4 fwd and pLSU-C-D rev primer pair (Marin *et al.*,
179 2005) using the Taq PCR mastermix (Qiagen, Germany). The cleaned-PCR product was purified (NucleoSpin
180 PCR clean-up kit, Macherey-Nagel, Germany) and sequenced (Wilmutte *et al.*, 1993). Sequences were merged
181 (HVDR Fragment Merger tool, Bell & Kramvis, 2013) and the final 16S-ITS sequence submitted to National
182 Center for Biotechnology Information, National Institute of Health, USA (NCBI).

hat formatiert: Schriftart: (Standard) Times New Roman, 10 Pt.

183 2.5.2 Isotope measurements

184 Stable isotope ratios of DO (expressed as δ¹⁸O_{DO}) were measured on a Delta V Advantage Isotope Ratio Mass
185 Spectrometer (IRMS; Thermo Fisher Scientific, Bremen, Germany) coupled to an automated equilibration unit
186 (Gasbench II). Measurements were carried out in continuous flow mode with a modified method by Barth *et al.*
187 (2004). Here the isolation of DO into a headspace relies on a helium extraction technique by Kampbell *et al.*
188 (1989) and Wassenaar and Koehler (1999). Different portions of laboratory air were injected into helium-flushed
189 Exetainers and used to correct obtained data sets for linearity and instrumental drift during each run. Here
190 laboratory air is defined to represent atmospheric oxygen with a ubiquitous value of 23.889 ‰ versus Vienna
191 Standard Mean Ocean Water (VSMOW) (Barkan and Luz, 2005). Data were normalized to this value.

hat formatiert: Schriftart: (Standard) Times New Roman, 10 Pt., Nicht Kursiv, Schriftfarbe: Automatisch

hat formatiert: Schriftart: (Standard) Times New Roman, 10 Pt., Nicht Kursiv, Schriftfarbe: Automatisch

192 ~~Data were normalized to laboratory air.~~

$$194 \delta = (R_{\text{sample}} / R_{\text{SMOW}} - 1) \quad (\text{Clark and Fritz, 1997})$$

196 To obtain ratio changes in per mille (‰), the δ values were multiplied by factor of 1000.

197 All samples were measured in triplicates and isotope values standard deviations (1σ) were less than 0.1 and 0.2 ‰
198 for δ¹⁸O_{H2O} and δ¹⁸O_{DO}, respectively.

199 **3 Results and discussion**

200 **3.1 On-site parameters**

201 The on-site parameters as displayed in Table 1 show a range of pH values between 6.1 and 8.6 in the cold season

202
203
204
205
206
207
208
209
210
211
212
213
214
215
216
217
218
219
220
221
222
223
224
225

Sampling point	Distance from spring (m)	pH	O ₂ (mg/L)	Temperature (°C)	Conductivity (mS/cm)	Alkalinity (mg/L)	Fe ²⁺ (mg/L)	Fe ³⁺ (mg/L)	Na ⁺ (g/L)	Ca ²⁺ (g/L)	SO ₄ ²⁻ (g/L)	Cl ⁻ (g/L)	U ⁶⁺ (µg/L)
Cold season													
E1a	0	6.1	2.3	19.5	16.8	820	6.6	0.4	2.5	1.2	2.1	4.4	170
E1b	0	6.5	3.4	19.3	16.4	828	6.6	0.4	2.5	1.2	2.2	4.5	170
E2	15	6.5	4.5	19.3	16.5	796	5.6	0.4	2.5	1.2	2.2	4.5	170
E3	45	6.7	5.8	17.5	16.8	790	5.7	0.4	2.5	1.2	2.2	4.5	170
E3.1	65	6.5	7.4	17.3	16.6	810	4.5	0.5	2.5	1.2	2.2	4.5	170
E4	85	7.1	8.0	16.2	16.9	804	3.9	0.6	2.5	1.2	2.2	4.5	170
E4.1	115	7.5	8.7	16.1	17.0	808	3.4	0.6	2.5	1.2	2.2	4.5	170
E5	145	7.9	8.9	15.2	16.8	804	0.9	0.8	2.4	1.2	2.2	4.5	170
E5.1	175	7.6	9.1	15.3	16.8	816	0.4	0.5	2.5	1.2	2.2	4.5	170
E6	205	7.9	9.5	14.1	16.9	760	0.2	0.1	2.5	1.2	2.2	4.5	170
E6.1	235	7.9	9.7	13.3	16.5	770	0.0	0.1	2.5	1.2	2.2	4.5	170
E7	265	8.0	10.1	12.3	16.6	760	0.0	0.1	2.4	1.1	2.2	4.5	170
E8	295	8.0	10.5	10.8	1.1	195	0.0	0.1	0.1	0.1	0.1	0.2	5.0
E9	300	8.6	11.0	7.4	0.5	160	0.0	0.1	0.0	0.1	0.0	0.0	0.4
Warm season													
E1a	0	6.3	3.6	21.3	16.3	874	6.9	0.0	2.4	1.1	2.2	4.5	190
E1b	0	6.4	3.9	21.2	16.4	850	6.7	0.1	2.5	1.1	2.2	4.4	190
E2	15	6.5	5.9	20.6	16.4	846	5.6	0.0	2.5	1.1	2.1	4.4	160
E3	45	6.6	6.6	21.6	16.4	814	4.0	0.0	2.4	1.1	2.2	4.4	160
E3.1	65	6.9	7.6	22.5	16.4	808	2.9	0.1	2.4	1.1	2.2	4.4	160
E4	85	7.2	8.2	22.7	16.4	826	1.5	0.1	2.5	1.1	2.2	4.4	160
E4.1	115	7.3	8.0	23.0	16.4	812	0.7	0.2	2.5	1.1	2.2	4.5	160
E5	145	7.4	8.1	24.0	16.4	786	0.1	0.1	2.4	1.1	2.2	4.5	160
E5.1	175	7.5	8.0	25.6	16.4	804	0.0	0.0	2.5	1.1	2.2	4.5	160
E6	205	7.5	8.1	25.7	16.4	796	0.0	0.0	2.5	1.1	2.2	4.5	160
E6.1	235	7.5	7.9	25.5	16.4	748	0.0	0.0	2.4	1.1	2.2	4.5	150
E7	265	7.5	8.1	24.9	16.4	742	0.0	0.0	2.5	1.1	2.2	4.5	150
E8	295	7.5	8.3	22.8	16.4	708	0.0	0.0	2.5	1.1	2.2	0.3	180
E9	300	8.0	8.8	16.8	0.8	238	0.0	0.0	0.1	0.1	0.0	0.0	1.0

226 **Table 1** On-site parameters; major ion concentrations and Fe(II) ~~ands well as~~ DO concentrations for the Espan
227 Spring. Note that values before the forward slash are for cold season and after the slash for warm season.

228 and between 6.3 and 8.0 in the warm season. The observed changes of the pH over the course of the spring are
229 mostly due to the constant degassing of CO₂ from the spring. Oxygen values rise-range from 2.3 mg/L to 11.0
230 mg/L in the cold season and from 3.6 mg/L to 8.8 mg/L in the warm season. Differences between the cold and
231 warm season are due to the fact that cold-water can hold-dissolve more dissolved-oxygen O₂ than warm water. The
232 general rise-increase in the amount of dissolved-oxygen DO over the course of the spring is due to a continuous
233 dissolution of atmospheric oxygen O₂ in the spring water and due to the impact of photosynthesis. ~~The w~~Water
234 temperatures ranged between 19.3- and 7.4°C in the cold season and between 21.-3 to-and 25.7°C in the warm
235 season. ~~The changes in temperature can be explained by an equilibration with the air temperatures thus dropping~~
236 ~~in the cold and rising in the warm season.~~ The conductivity remained relatively stable over the course of the spring
237 and only showed minor differences between the cold and warm season. The same applies to the alkalinity. The
238 behaviourbehavior of the Fe(II) and Fe(III) are-is described in section 3.5. Values of major eations-and-anions-ions
239 (Cl⁻, SO₄²⁻, NO₃⁻, Na⁺, K⁺, Ca²⁺ and Mg²⁺) remained constant over the course of the spring and show no differences
240 between the cold and warm season.

241 3.2 Precipitation calculations

242 Precipitating mineral phases as determined with Phreeqc showed that the dominant phase at all measurement
243 points is-was Hematite (Fe₂O₃) (Supplementary Information Table S1 and S2). Additionally, Goethite (α-
244 FeO(OH)), Ferrihydrite (Fe(OH)₃), Siderite (FeCO₃) and K-Jarosite (KFe³⁺₃(OH)₆(SO₄)₂) as well as CaCO₃ and
245 Rhodochrosite (MnCO₃) showed elevated SI values to-enableand indicated precipitation.

246 3.3 Bacterial contents

247 Confocal Laser scanning microscopy (CLSM) showed that only the samples from Site E4.1 have photosynthetic
248 organisms in significant quantities during the cold period. The photosynthetic community in this biofilm was
249 dominated by cyanobacteria, with very few eukaryotic algae (Fig. -2). Lyngby was observed along the sides of the
250 fast-flowing stream on the smooth hard canal section at E2, however, the loosely built Lyngbya sp. mats were only
251 observed in the wider, shallower sections from sampling sites E3 to E5, and predominating between sites E3.1 and
252 E4.1. The Lyngbya sp. filaments were not encrusted by oxidized iron as identifiedproven by light microscopy. As
253 these are simple cyanobacterial mats on top of loose iron oxides, with no additional microbial layers beneath them,
254 the bubbles are presumably oxygen generated during photosynthesis (Supplementary Information Fig. 1)
255 ▲

hat formatiert: Tiefgestellt

hat formatiert: Tiefgestellt

hat formatiert: Hochgestellt

hat formatiert: Tiefgestellt

hat formatiert: Hochgestellt

hat formatiert: Tiefgestellt

hat formatiert: Hochgestellt

hat formatiert: Hochgestellt

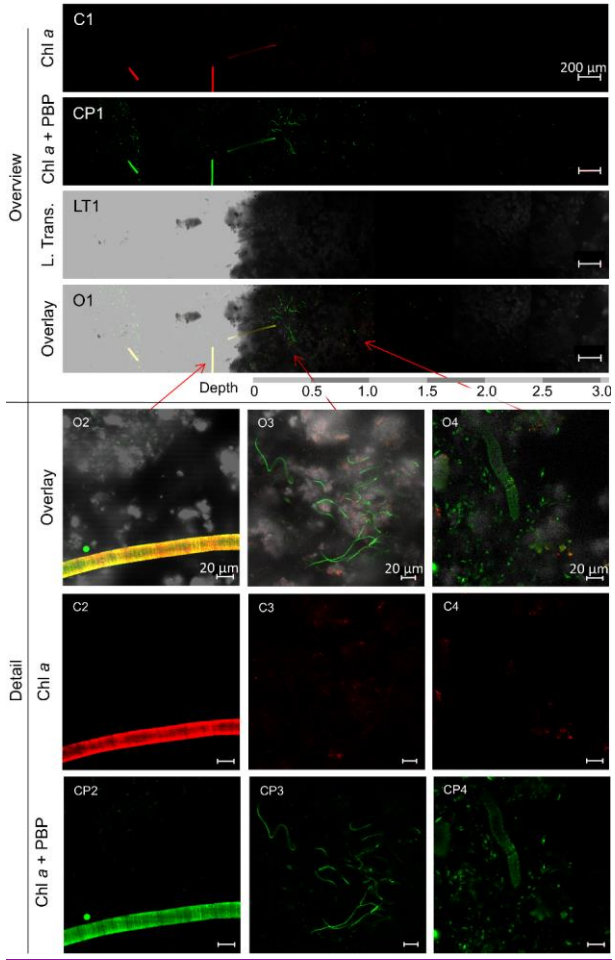
hat formatiert: Hochgestellt

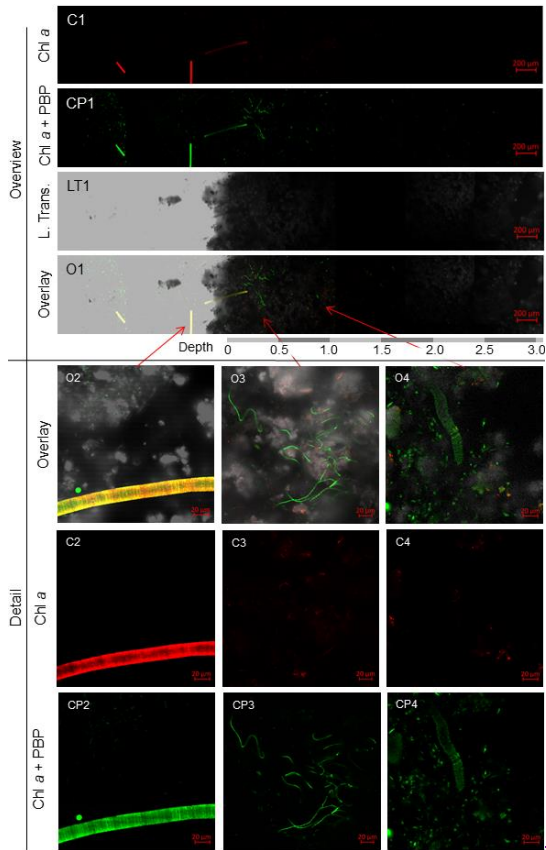
hat formatiert: Hochgestellt

hat formatiert: Hochgestellt

hat formatiert: Schriftart: (Standard) Times New Roman, 10 Pt.

hat formatiert: Englisch (Vereinigte Staaten)





257

258

259

260

261

262

263

Figure 2 CLSM images of mat sample E4.1. Overview: images of the cross-section of the top 3 mm of the biofilm with the *cChl-a* (C1) and *ehchl-a* plus PBP (CP1) fluorescence profile, complemented by a laser transmission picture (LT1) and the superimposed image (O1). **Detail:** Superimposed images (O2/3/4) of *cChl-a* (C2/3/4) and *cChl-a* plus PBP (CP2/3/4) fluorescence and laser transmission (not shown) of distinct organisms found in the bio mat. **O2:** eukaryotic algae. **O3:** Possible *Klisinema*- or *Persinema*-like sp. and a unicellular cyanobacterium. **O4:** *Lynbya* -like sp. and a unicellular cyanobacterium.

264

265

266

267

268

269

270

271

Most of the cyanobacteria and all eukaryotic algae were located in the topmost 1.2 mm of the biofilms (Fig. 2 O1). Close-up images show eukaryotic algae (Fig. 2.O2), thin filamentous cyanobacteria, possibly *Persinema* sp. or *Klisinema* sp. (Fig. 2.O3) and *Lynbya* sp. (Fig. 2.O4). All pictures of the top layers of this sample site show an abundance of unidentified unicellular cyanobacteria, while images from the other sample sites show very few photosynthetic organisms at all ([Supplementary Information Fig. 2supplementary-material](#)). In order to determine the identity of the predominant cyanobacterial species isolated from the E4.1 enrichment cultures, a determination key ([Komárek und Anagnostidis, 2005](#)) was used to compare particular features of an isolate to those already in the literature for specific cyanobacterial species ([Komárek und Anagnostidis, 2005](#)).

hat formatiert: Schriftart: Kursiv

hat formatiert: Schriftart: Kursiv

272 Note that enrichment cultures for samples E2 and E3 did not yield enough material for cyanobacterial
273 determination after 5 weeks in culture.

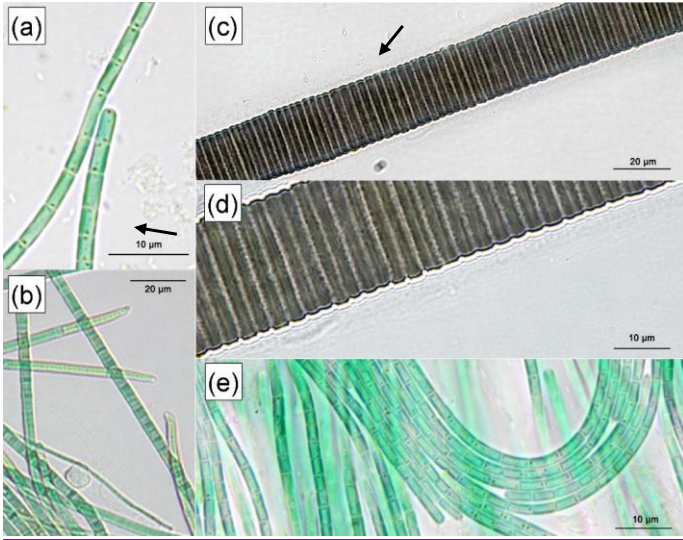
274 The red-brown filamentous strain (Fig. 3, c, & d) exhibits single filaments, without false branching, that are 30.9
275 to 38.2 μm wide (Table 2), with a firm, 9.5 to 14 μm thick sheath. The trichomes and single cells are 21.5 to 24.2
276 μm wide and 1.5 to 4.1 μm long (Table 2), are red-brown in colour and constricted at the cross-walls. Based on
277 these characteristics, the species was attributed to the cyanobacterial genus *Lyngbya*.

278

	Filament length	Filament width (μm)	Cell width (μm)	Cell length (μm)
<i>Lyngbya sp.</i>	Indeterminate	30.9 – 38.2	21.5 – 24.2	1.5 – 4.1
<i>Klisinema sp.</i>	Indeterminate	3.9 – 7.6	12 – 4.5	0.3 – 0.4
<i>Persinema. sp</i>	Indeterminate		0.5 – 1.8	2.7 – 4.7

279 **Table 2** Filament and cell dimensions of the proposed cyanobacterial species.

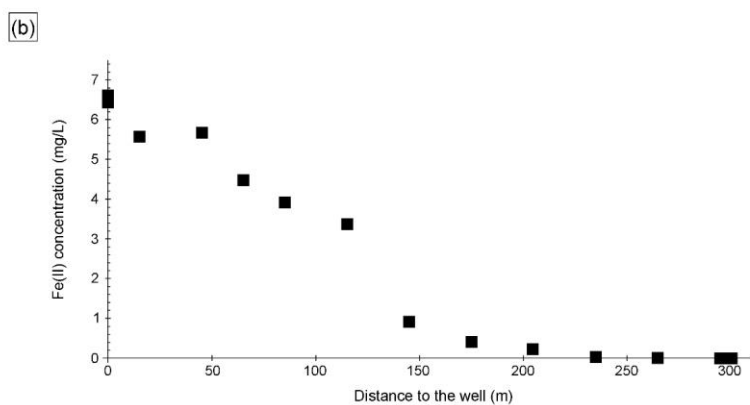
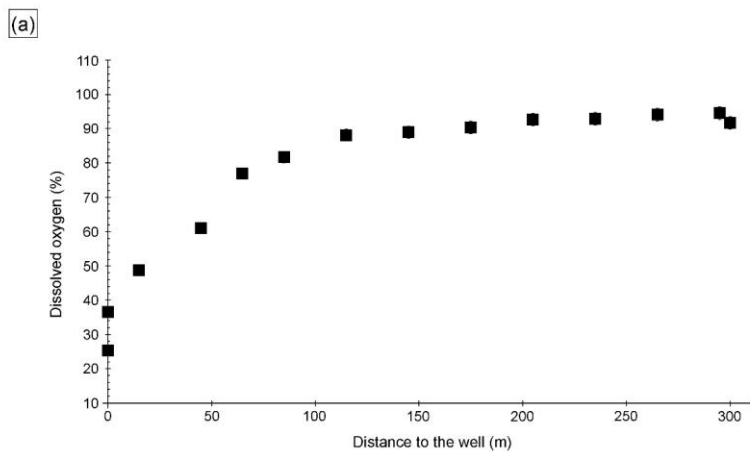
280 The blue-green filamentous strain (Fig. 3, b) produces single filaments, without false branching, that are 3.9 ~~to~~
281 7.6 μm wide (Table 2) with a firm, 2.7 ~~to~~ 3.1 μm thick sheath. The trichomes and single cells are 1.2 ~~to~~ 4.5 μm
282 wide and 0.3 ~~to~~ 0.4 μm long (Table 2), blue-green in colour, ~~without~~ ~~no~~ constriction at the cross-walls. The
283 terminal cells in mature filaments are conical, elongated and bent to one side, corresponding to those of the
284 *Klisinema* genus recently described by Heidari et al. (2018). The thin, naked pale green filaments (Figure 3a & e)
285 resembled those of *Persinema komarekii* (Heidari et al., 2018) with apical cells flattened at the end. In contrast to
286 the observations of Heidari et al. (2018), we observed terminal aerotopes. This species was purified in culture and
287 the 16S-ITS (NCBI accession number: MT708471) sequence confirmed its identity to *Persinema komarekii*
288 (MF348313).



289
 290 **Figure 3** Light Micrographs of the predominant isolates from sample E4.1: a) Single filament of *Persinema sp.*,
 291 arrow indicates aerotopes. b) Biofilm of *Klisinema sp.* interspersed with *Persinema sp.* (arrow) c) *Lyngbya sp.*,
 292 filament d) *Lyngbya sp.* sheath detail, E: Biofilm of *Persinema sp.*

293 **3.4 Dissolved oxygen (DO)**

294 The DO concentration in the Espan System was lowest at the faucet in the Pavilion (sampling point E1a) with a
 295 saturation of 25.3 % (2.3 mg/L) (Fig. 4a). Over the next following 100 meters DO saturation rose-increased to 88.1
 296 % (8.7 mg/L) in sampling point E4.1. Afterwards the saturation continually rose-increased to 94.6 % (11.0 mg/L)
 297 in point E8. From an initial depth of 435 meters with the abundance of reduced species such as Fe(II) and Mn(II),
 298 the low DO content in sampling point E1a was expected. In and in the further course, more atmospheric oxygen
 299 was able to dissolve. In addition, gas Bubbles-bubbles were observed in association with the *Lyngbya* mats. They
 300 were most prominent at sample site E4.1 and indicate a significant contribution of O₂ from daytime photosynthesis.
 301 However, saturation with DO was not reached during neither of the sampling campaigns.
 302



303
 304 **Figure 4** a) Dissolved oxygen (%) and b) Fe(II) concentrations over the course of the Espan [System in an example](#)
 305 [graph for the \(cold season\)- In February](#). The error for DO was 2 % and for Fe(II) it was 0.06 mg/L. Errors are
 306 within symbol size.

307 **3.5 Fe(II) and Fe(III)**

308 The Fe(II) content was highest at the faucet with 6.6 mg/L while its lowest content was below instrument precision.
 309 at sampling point E9 at 300 meters from the source (Fig. 4b). Fe(II) concentrations decreased constantly over the
 310 stream course and were accompanied by increases in DO saturation (Fig. 4a). The decrease in Fe(II) could have
 311 been caused by three major processes:

- 312 (1) Oxidation of Fe(II) to form ferric iron minerals such as ferrihydrite, hematite and goethite
 313 (2) Precipitation of Fe(II) minerals such as the iron carbonate siderite (FeCO₃) and/or an amorphous ferrous silicate
 314 phase or
 315 (3) Adsorption of Fe(II) on already formed iron minerals.

316
317 All three possibilities seem plausible when taking into consideration the saturation indices of ferric iron minerals,
318 goethite, ferrihydrite and hematite precipitate at all sampling points in the system (Köhler et al. 2020). These
319 calculations furthermore show that siderite can precipitate in almost all sampling points while iron-silicate minerals
320 are unlikely to precipitate. Therefore, adsorption of Fe (II) onto minerals ~~should-is-be-also~~ a possible mechanism
321 in the Espan System. Such adsorption of Fe(II) onto (oxyhydr)oxides was shown to typically occur under neutral
322 conditions and should increase with rising pH (Zhang et al.,1992; Liger et al., 1999; Appelo et al., 2002; Silvester
323 et al., 2005). ~~Moreover, of large amounts of sulphate and chloride with average values of 2.2 and 4.5 g/L, may have~~
324 ~~been responsible for maintaining~~ The observed high dissolved Fe(II) contents of the spring system at circum-
325 neutral pH, ~~and rising despite rising~~ DO concentrations, ~~can be explained by the occurrence of large amounts of~~
326 ~~sulphate (~2.2 g/L) and chloride (~4.5 g/L). These~~ Such elevated Cl^- and SO_4^{2-} contents ~~parameters~~ can delay
327 abiotic Fe(II) oxidation (Millero, 1985).

hat formatiert: Hochgestellt

hat formatiert: Tiefgestellt

hat formatiert: Hochgestellt

328
329 Dissolved Fe(III) was highest (0.8 mg/L) at sampling point E5 after 145 m and lowest (0.05 mg/L) at sampling
330 point E7 after 265 m flow distance from the spring. The values initially ~~rose-increased~~ from 0.4 mg/L in E1a to a
331 maximum of 0.8 mg/L in point E5 (+/- 0.03 mg/L) and then decreased to their lowest value in sampling point E7.
332 The solubility of iron oxides in natural systems at a circum-neutral pH and under aerobic conditions is generally
333 very low (Cornell and Schwertmann, 2003) with values of the solubility product (K_{sp}) between 10^{-37} and 10^{-44}
334 (Schwertmann, 1991). However, Fe(III) could still be detected in the water, thus showing that its dissolution was
335 possible. The dissolution of iron oxides can occur through several pathways including as protonation, reduction
336 and complexation that create Fe(III) cations, Fe(II) cations as well as Fe(II) and Fe(III) complexes (Schwertmann,
337 1991; Cornell and Schwertmann, 2003). Both the protonation as well as the reduction would lead to the formation
338 of dissolved Fe(II). A steep increase in dissolved Fe(III) at 145 m downstream of the spring (from 0.5 mg/L to
339 0.8 mg/L) also indicates ~~indicated~~ acceleration of this process. One reason for this increase could be available
340 organic matter. However, further analyses are needed to verify this interpretation.

341 3.6 $\delta^{18}O_{DO}$

342 Figure 5 a) and b) show $\delta^{18}O_{DO}$ values over the course of the spring for the cold and warm seasons, respectively.
343 The curves are divided into two zones for the cold season and three zones for the warm season. ~~A zone was defined~~
344 ~~by the increase or decrease of the $\delta^{18}O_{DO}$ values.~~

345 Zone 1

346 In the cold season, zone 1 extended from sampling point E1a to point E4. In these first 85 meters, the $\delta^{18}O_{DO}$ ~~rose~~
347 ~~increased~~ from a value of +23.7 ‰ at the faucet (E1a) to + 25.7 ‰ at E4. In the warm season, zone 1 extended
348 from E1a to E2 ~~at with~~ only 15 m distance from the spring. In this zone the values ~~rose-increased~~ from + 23.4 ‰
349 at the faucet to a maximum value of + 24.7 ‰ at E2. In both seasons, $\delta^{18}O_{DO}$ values at E1a were below the value
350 expected for atmospheric equilibration (+ 24.6 ‰). At first sight such ~~light- ^{16}O -enriched~~ $\delta^{18}O_{DO}$ values would
351 suggest photosynthetic input of DO. However, the water ~~did not have any~~ originated from greater depths without
352 any exposure to contact with light and thus any photosynthetic influence can be ruled out.

hat formatiert: Hochgestellt

353 The occurrence of $\delta^{18}O_{DO}$ values below + 24.6 ‰ in groundwater has been described in the literature (Wassenaar
354 and Hendry, 2007; Smith et al., 2011; Parker et al., 2014 and Mader et al., 2018) and several explanations for this

355 phenomenon have been suggested (Wassenaar and Hendry, 2007; Smith et al., 2011; Parker et al., 2014 and Mader
356 et al, 2018). These include:
357 (1) possible transfer of photosynthetic or diffusive oxygen into the shallow aquifer (Smith et. al; 2011; Parker et
358 al., 2014; Mader et al., 2018),
359 (2) radial oxygen loss of plant roots (Teal and Kanwisher, 1966; Michaud and Richardson, 1989; Caetano and
360 Vale, 2002; Armstrong and Armstrong, 2005b)
361 (3) radiolysis of water (Wassenaar and Hendry, 2007) and
362 (4) kinetic gas transfer (Benson and Krause, 1980; Knox et al. ,1992; Mader et al. 2017)
363 Explanations (1) and (2) are very unlikely in the Espan Spring, because the water originates from a depth of 435
364 meters below ground, through pipes that presumably prevent any exchange with surface water or possible impacts
365 of plant roots. It should however be noted that water from the Espan Spring contains up to 170 µg/L of uranium
366 from easily soluble uranium compounds that are commonly encountered in the Buntsandstein formations (Büttner
367 et al. 2006; Meurer and Banning, 2019). The geogenic radiation in the area is ~~additionally~~ rather high because of
368 the high uranium content in the Variscian bedrocks of the area (Schwab, 1987; Büttner et al., 2006). Because of
369 this, radiolysis could be a possible explanation for the unexpected low $\delta^{18}\text{O}_{\text{DO}}$ values. Kinetic gas transfer of
370 atmospheric oxygen during transport in the pipes or at the faucet might ~~be the most likely~~ another explanation,
371 since the sample in E1a is strongly DO undersaturated. During non-equilibrium gas exchange the kinetically faster
372 ^{16}O would cause $\delta^{18}\text{O}_{\text{DO}}$ ~~values lighter than~~ below ± 24.6 ‰ until equilibrium ~~is~~ establisheds (Benson and Krause,
373 1980; Knox et al. ,1992, Mader et al. 2017).
374

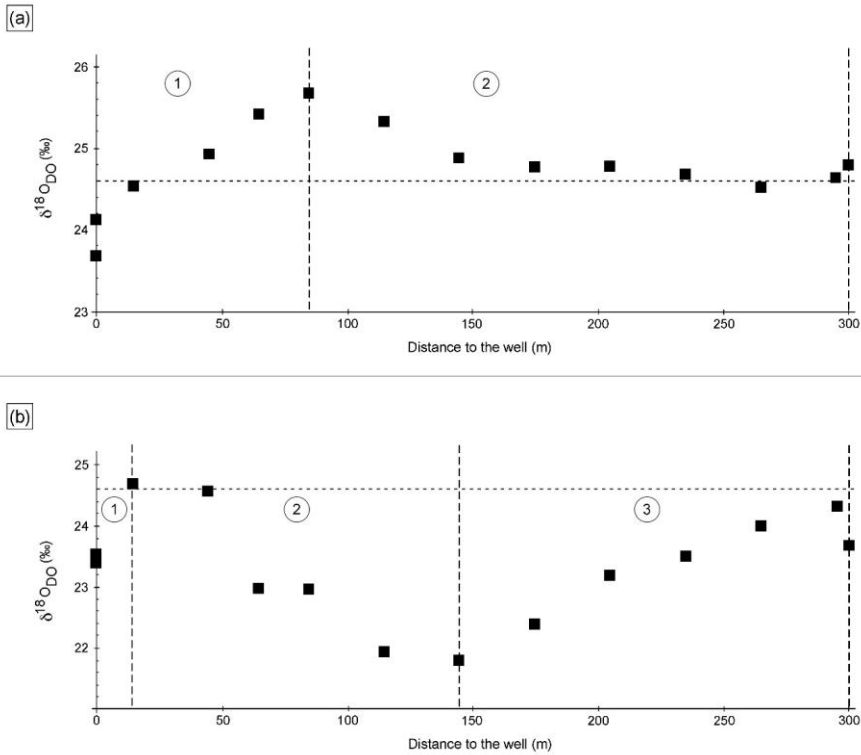
hat formatiert: Schriftart: (Standard) Times New Roman, 10 Pt.

hat formatiert: Schriftart: (Standard) Times New Roman, 10 Pt.

hat formatiert: Schriftart: (Standard) Times New Roman, 10 Pt.

hat formatiert: Schriftart: (Standard) Times New Roman, 10 Pt, Englisch (Vereinigte Staaten)

hat formatiert: Englisch (Vereinigte Staaten)



375
 376 **Figure 5** δ¹⁸O_{DO} in the cold season a) and the warm season b) over the course of the Espan [Spring and stream](#)
 377 system with the atmospheric equilibrium value of + 24.6 ‰ marked by the horizontal line. Dashed vertical lines
 378 show borders of the different zones of the [curves fields](#) labelled with 1, 2 and 3. The symbol size is larger than the
 379 error bars.

380 Increases in δ¹⁸O_{DO} values in zone 1 were accompanied by increases in DO (Fig. 6a). In the cold season, a strong
 381 positive correlation was evident between points E1a and E4. However, in the warm season, the same correlation
 382 could only be observed between points E1a and E2 (Fig. 6b). ~~Through e~~Equilibration with the atmosphere, ~~this~~
 383 ~~trend~~ would be reasonable [explanation for this trend](#) until atmospheric equilibration was reached between point
 384 E2 and E3. However, the δ¹⁸O_{DO} values, at least in the cold season, increased above this threshold to a value of
 385 + 25.7 ‰. [This shows that another process in addition to atmospheric equilibration must have influenced the](#)
 386 [δ¹⁸O_{DO} values in zone 1.](#) In the warm season, ~~this was less~~ evident, ~~and~~ the [isotope atmospheric equilibrium value](#)
 387 was only marginally exceeded and remained within the range of the analytical uncertainties. ~~This shows that~~
 388 ~~another process in addition to atmospheric equilibration must have influenced the δ¹⁸O_{DO} values in zone 1.~~

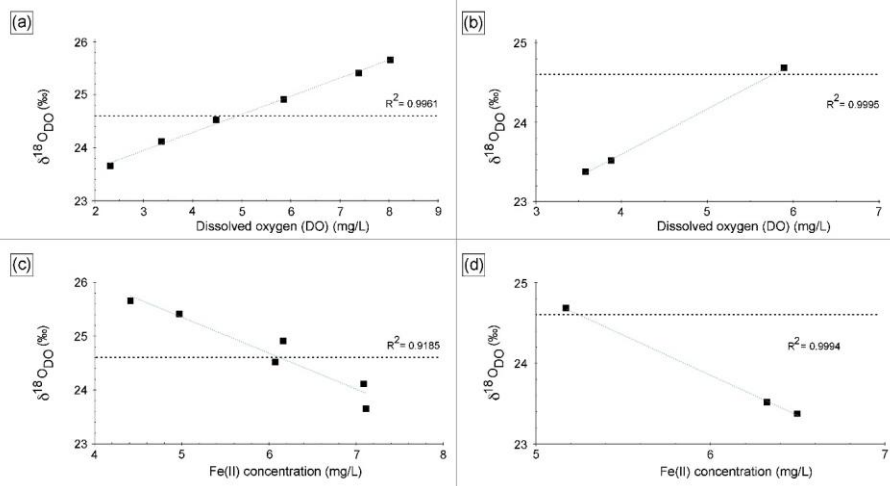


Figure 6 Correlation between $\delta^{18}\text{O}_{\text{DO}}$ and DO over the course of the spring for zone 1 in the cold season a) and the warm season b). Correlation between $\delta^{18}\text{O}_{\text{DO}}$ and Fe(II) contents over the course of the stream for zone 1 in the cold season c) and the warm season d).

Even though these processes consume DO, both respiration and iron oxidation could be responsible for this trend when assuming that they influence the $\delta^{18}\text{O}_{\text{DO}}$ values, while DO concentrations are constantly replenished by the atmosphere. **Notably, a** direct negative correlation between Fe(II) concentrations and $\delta^{18}\text{O}_{\text{DO}}$ values between point E1a and E4 was evident for cold season samples and in point E1a and E2 for warm season samples as shown in Figure 6c and d. This correlation between Fe(II) and $\delta^{18}\text{O}_{\text{DO}}$ in the Espan **S**system corresponds with the experimental observations of Oba and Poulson (2009), as well as those of Pati et al. (2016). These studies demonstrate that Fe oxidation leads to increases in $\delta^{18}\text{O}_{\text{DO}}$ values due to preferential consumption of ^{16}O . The increase in $\delta^{18}\text{O}_{\text{DO}}$ due to iron oxidation in a natural system, which is constantly supplied with fresh oxygen, indicates that Fe(II) oxidation must be **the a** dominant control on $\delta^{18}\text{O}_{\text{DO}}$ in the first 85 meters of the stream in the cold season and in the first 15 meters in warm season. It also implies that the direct impact of oxygen addition is subordinate in terms of DO stable isotope changes. **This is shown by as the results show that iron oxidation is being the dominant factor that controlling the $\delta^{18}\text{O}_{\text{DO}}$ values, even though oxygen is constantly supplied from the atmosphere.**

Zone 2

In the cold season, zone 2 extended from sampling point E4 to point E9 **and with** only minor variations in $\delta^{18}\text{O}_{\text{DO}}$ **could be found**. In this zone, the $\delta^{18}\text{O}_{\text{DO}}$ decreased from + 25.7 ‰ in sampling point E4 to values around atmospheric equilibrium with + 24.5 ‰ in E7 and + 24.8 ‰ in the Pegnitz River (Fig. 5a).

In the warm season, zone 2 extended from sampling point E2 to point E5 at 145 meters **distance** from the spring. In this zone the values decreased from + 24.7 ‰ to a minimum value of + 21.8 ‰ in **sampling** point E5 (Fig. 5b). This decrease in $\delta^{18}\text{O}_{\text{DO}}$ values can be explained by (1) a decrease of the impact of iron oxidation on the $\delta^{18}\text{O}_{\text{DO}}$

416 values and (2) a rising impact of atmospheric or photosynthetic oxygen. Even though a decrease in Fe(II) values
417 was still evident between E4 and E7 in the cold season, as well as between E2 and E5 in the warm season, it is
418 possible that the decrease was not caused by Fe(II) oxidation and subsequent precipitation as iron oxides.

419 ~~Alternatively~~Alternatively, the decrease could have been caused by adsorption of dissolved Fe(II) onto already
420 existing iron oxides such as goethite, ferrihydrite and hematite (Zhang, et al., 1992; Liger et al., 1999; Appelo et
421 al., 2002; Silvester et al. 2005). Because adsorbed Fe(II) is very resistant to oxidation (Park and Dempsey, 2005)
422 the impact of iron oxidation on the $\delta^{18}\text{O}_{\text{DO}}$ values would have decrease.

423 ~~The question remains why an increased adsorption would occur specifically downstream of points E2 and E4.~~
424 ~~No~~significant changes in the water chemistry were evident and it can be assumed that after sampling point E2
425 (warm season) or E4 (cold season), a critical value is/was exceeded with enough Fe(II) having been adsorbed onto
426 iron oxides. ~~that In this case,~~ iron oxidation --- while probably still taking place at small rates--- is no longer the
427 an important factor dominating the $\delta^{18}\text{O}_{\text{DO}}$ values. Downstream of point E2 and E4 oxygen addition by the
428 atmosphere or by photosynthesis would ~~thus become the dominating factor~~ more important.

429 ~~Because of~~Intensive growth of cyanobacterial and algal mats (~~Fig. 1f~~) were observed between point E3.1 and E5 in
430 the cold season and between E3 and E5 in the warm season (~~Fig. 1f~~). Because of this growth it can be postulated
431 that, in addition to the atmospheric O_2 input, the $\delta^{18}\text{O}_{\text{DO}}$ values were also influenced by addition of
432 photosynthetically produced oxygen. While this effect should be less pronounced in the cold and darker season, a
433 stronger influence of photosynthetic oxygen on the $\delta^{18}\text{O}_{\text{DO}}$ values ~~should/would be expected be possible~~ in the
434 warm season with higher light intensity. Such Considerable growth of photosynthetic organisms in the Espan
435 System is not surprising with iron being an important micronutrient (Andrews et al., 2003).

436 The fact that photosynthesising organisms seem to preferentially grow and impact the $\delta^{18}\text{O}_{\text{DO}}$ values between
437 sampling point E3 and E5 may be due to the availability of Fe(II). In addition, ~~The~~ growth could also be due
438 controlled by ~~to~~ changes in the pH or other environmental influences, with the site being located in a public park
439 with the associated perturbations. Cyanobacteria, especially aquatic strains prefer a neutral to alkaline pH (Brock,
440 1973) and the shift to higher pH values in this zone could be one of the main factors that drive increased supply of
441 cyanobacterial O_2 . For instance, *Lyngbya* spp. are diazotrophic cyanobacteria, capable of fixing nitrogen during
442 the night or dawn low availability of light, when local oxygen levels are low (Stal, 2012, p. 102). This Oxygen
443 released through oxygenic photosynthesis would immediately react with Fe(II) thereby lowering and lower the
444 partial pressure of oxygen around the organisms in a slow flowing stream. This could also possibly favoring
445 biological nitrogen fixation as well as and limiting carbon loss by reducing photorespiration. Additionally, the
446 reduced oxygen partial pressure induced by Fe(II) oxidation may minimize the oxygenase activity of ribulose 1,5-
447 biphosphate carboxylase/oxygenase (Rubisco), thereby favoring CO_2 -fixation (Stal, 2012, p. 113).

448 ▲
449 A screening of microbial ecology in several iron-rich circum-neutral springs and experiments with the
450 cyanobacterium *Synechococcus* PCC 7002 (Swanner et al. 2015a) revealed that many cyanobacteria show optimal
451 growth between 0.4 – 3.1 mg/L Fe(II) and that concentrations above 4.5 mg/L become growth-limiting. The iron
452 concentrations between point E3.1 and E5 in the cold season and E3 and E5 in the warm season are thus
453 approximately in the range of optimal cyanobacterial growth. In order to establish a clear correlation between the
454 iron concentration and the decrease in $\delta^{18}\text{O}_{\text{DO}}$ values, experiments would need to be carried out with the organisms
455 found in the Espan System. These have so far have not been assessed for their behaviour under variable iron
456 concentrations.

hat formatiert: Englisch (Vereinigte Staaten)

457 *Zone 3*

458 In the warm season, zone 3 extended from sampling point E5 to point E8. In this zone the $\delta^{18}\text{O}$ values rose again
459 from + 21.8 ‰ to + 24.3 ‰ (Fig. 5B). The renewed increase in values can be explained by the influence of iron
460 oxidation, respiration and a decrease in photosynthetic activity. Because Fe-contents only decreased marginally,
461 it can be assumed that decreases in photosynthetic activities are responsible for increase in the $\delta^{18}\text{O}$ values. This
462 matches our observations that downstream of point E5, only little or no photosynthetic growth ~~could be~~
463 ~~observed~~took place. Oxygen that would dissolve in the water after point E5 would thus most likely stem from the
464 atmosphere. This would also explain the approach to the equilibrium value of + 24.6 ‰. Reasons for the observed
465 decrease in cyanobacteria are however not clear ~~however, they~~and may include changes in temperature, light
466 intensity and shifts in nutrient availability.

467 The temperature did not change significantly in this part of the watercourse and is therefore unlikely to have caused
468 a decrease in photosynthetic oxygen production. In contrast, reduced light exposure ~~can in fact be~~could have been
469 responsible as downstream of point E5 trees shade the ~~spring~~water course. A decrease in nutrient availability is
470 difficult to determine because nitrate and phosphate were below the detection limit in the entire spring. Iron
471 starvation could also be a possible reason for the decrease in activity because only ~0.005 mg/L Fe(II) was left in
472 the system in the ~~later~~lowest course of the stream. ~~In order to outline these processes future studies should target~~
473 ~~laboratory experiments with the photosynthetic organisms found.~~

474 4 Conclusions

475 Our study is the first systematic analysis of $\delta^{18}\text{O}_{\text{DO}}$ values as a function of iron contents and oxygenic
476 photosynthetic biofilms in a natural iron-rich spring. We were able to confirm from field samples that Fe-oxidation
477 leads to increases in $\delta^{18}\text{O}_{\text{DO}}$ values even though oxygen was constantly replenished by atmospheric input. As soon
478 as photosynthetic oxygen is produced in the system, the effect of iron oxidation on the $\delta^{18}\text{O}_{\text{DO}}$ values becomes
479 negligible and can no longer be detected. The fact that photosynthesis has a strong impact on the $\delta^{18}\text{O}_{\text{DO}}$ values in
480 specific areas of the system may be controlled by high Fe contents of the system. Similar iron-rich springs show
481 optimal growth rates of cyanobacteria in the range of 0.4 – 3.1 mg/L Fe(II). The presented $\delta^{18}\text{O}_{\text{DO}}$ values showed
482 that photosynthetic activity is also strongest in the Espan System within this range of concentrations.

483 To what extent the changing Fe concentrations (Fe(II)/Fe(III)) influence the growth of cyanobacteria and algae
484 occurring in the Espan System, requires further investigation. This would ideally include isolating the organisms
485 from the water course and studying them under varying experimental levels of Fe, pH and temperature while
486 monitoring the $\delta^{18}\text{O}_{\text{DO}}$ of the system. ~~Further field studies with organic material from the stream bed in~~
487 ~~combination with stable carbon isotopes would be promising to narrow down processes for carbon and oxygen~~
488 ~~budgets in this environment.~~

489 5 Author contribution

490 Inga Köhler, David Piatka and Johannes Barth carried out the sample collection and water analysis for on-site and
491 isotope data. Raul Martinez carried out the calculation of the saturation index. Michelle Gehringer, Achim

492 Herrmann and Arianna Gallo performed the analysis and interpretation of cyanobacteria and algae data. Inga
493 Köhler prepared the manuscript with contributions from all co-authors

494 6 Acknowledgements

495 Funding for this project was made available by the German Research Foundation (DFG) in the Project IsoDO (BA
496 2207/15-1) awarded to Johannes Barth and GE2558/3-1 & GE2558/4-1 awarded to Michelle Gehringer. We also
497 thank Christian Hanke, Marlene Dordoni and Marie Singer for help with sampling and analyses. The authors
498 declare that they have no conflict of interest.

499 References

500 Andrews, S. C., Robinson, A. K., and Rodríguez- Quiñones, F.: Bacterial iron homeostasis, FEMS Microbiol.
501 Rev., 27, 215-237, [https://doi.org/10.1016/S0168-6445\(03\)00055-X](https://doi.org/10.1016/S0168-6445(03)00055-X), 2003.

502

503 Appelo, T., Van der Weiden, M. J., Tournassat, C., and Charlet, L.: Surface Complexation of Ferrous Iron and
504 Carbonate on Ferrihydrite and the Mobilization of Arsenic, Environ. Sci. Technol., 36, 3096-3103,
505 <https://doi.org/10.1021/es010130n>, 2002.

506

507 Armstrong, W., and Armstrong, J.: Stem photosynthesis not pressurised ventilation is responsible for light-
508 enhanced oxygen supply to submerged roots of alder (*Alnus glutinosa*), Ann. Bot., 96, 591-612,
509 <https://doi.org/10.1093/aob/mci213>, 2005.

510

511 Barth, J. A. C., Tait, A., and Bolshaw, M.: Automated analyses of O-18/O-16 ratios in dissolved oxygen from 12-
512 mL water samples, Limnol. Oceanogr. Methods., 2, 35-41, <https://doi.org/10.4319/lom.2004.2.35>, 2004.

513

514 Bell, T. G., and Kramvis, A.: Fragment Merger: An Online Tool to Merge Overlapping Long Sequence
515 Fragments, Viruses, 5, 824-833, <https://doi.org/10.3390/v5030824>, 2013.

516

517 Benson, B. B., and Krause D.: The concentration and isotopic fractionation of gases dissolved in freshwater in
518 equilibrium with the atmosphere. 1. Oxygen, Limnol. Oceanogr., 25, 662-671,
519 <https://doi.org/10.4319/lo.1980.25.4.0662>, 1980.

520

521 Büttner, G., Stichler, W., and Scholz M.: Hydrogeochemische Untersuchungen in den Forschungsbohrungen
522 Lindau 1 und Spitzeichen 1 (Fränkisches Bruchschollenland), Geol. Bavar., 109, 105-124, 2006.

523

524 [Bjrzer, F.: Eine Tiefbohrung durch das mesozoische Deckgebirge in Fürth in Bayern.- Zbl. Min. etc., Abt. B.: 425-](#)
525 [433. Stuttgart, 1936.](#)

526

527 Brock T. D.: Lower pH limit for the existence of blue-green algae: evolutionary and ecological implications,
528 Science, 179, 480-483, <http://doi.org/10.1126/science.179.4072.480>. 1973.

hat formatiert: Schriftart: (Standard) Times New Roman, 10 Pt., Deutsch (Deutschland)

hat formatiert: Schriftart: (Standard) Times New Roman, 10 Pt.

hat formatiert: Schriftart: (Standard) Times New Roman, 10 Pt., Deutsch (Deutschland)

hat formatiert: Schriftart: (Standard) Times New Roman, 10 Pt.

hat formatiert: Schriftart: (Standard) Times New Roman, 10 Pt., Deutsch (Deutschland)

hat formatiert: Schriftart: (Standard) Times New Roman, 10 Pt., Englisch (Vereinigte Staaten)

hat formatiert: Englisch (Vereinigte Staaten)

hat formatiert: Schriftart: (Standard) Times New Roman, 10 Pt., Englisch (Vereinigte Staaten)

hat formatiert: Englisch (Vereinigte Staaten)

529
530 Caetano, M., and Vale, C.: Retention of arsenic and phosphorus in iron-rich concretions of Tagus salt marshes,
531 Mar. Chem., 79, 261-271, [https://doi.org/10.1016/S0304-4203\(02\)00068-3](https://doi.org/10.1016/S0304-4203(02)00068-3), 2002.
532 Clark, I. D. and Fritz, P. (Eds.): Environmental Isotopes in Hydrogeology, CRC Press/Lewis, Boca Raton, USA,
533 1997.
534
535 Cornell, R. M. and Schwertmann, U. (Eds.): The Iron Oxides: Structure, Properties, Reactions, Occurrences and
536 Uses, Wiley-VCH Verlag, Weinheim, Germany, 2003.
537
538 Eisenstadt, D., Barkan, E., Luz, B., and Kaplan, A.: Enrichment of oxygen heavy isotopes during photosynthesis
539 in phytoplankton, Photosynth. Res., 103, 97-103, <https://doi.org/10.1007/s11120-009-9518-z>, 2010.
540
541 Gammons, C. H., Henne, W., Poulson, S. R., Parker, S. R., Johnston, T. B., Dore, J. E., and Boyd, E. S.: Stable
542 isotopes track biogeochemical processes under seasonal ice cover in a shallow, productive lake, Biogeochemistry,
543 120, 359–379, <https://doi.org/10.1007/s10533-014-0005-z>, 2014.
544
545 Gehringer, M. M., Pengelly, J. J. L., Cuddy, W. S., Fieker, C., Foster, P. I., and Neilan, B. A.: Host selection of
546 symbiotic cyanobacteria in 21 species of the Australian cycad genus: Macrozamia (Zamiaceae), Mol. Plant.
547 Microbe. Interact., 23, 811-822, <https://doi.org/10.1094/MPMI-23-6-0811>, 2010.
548
549 Guy, R. D., Fogel, M. L., and Berry J. A.: Photosynthetic fractionation of the stable isotopes of oxygen and
550 carbon, Plant Physiol., 101, 37–47, <https://doi.org/10.1104/pp.101.1.37>, 1993.
551
552 Heidari, F., Zima, J., Riahi, H., and Hauer, T.: New simple trichal cyanobacterial taxa isolated from radioactive
553 thermal springs, Fottea. Olomouc., 18, 137-149, <https://doi.org/10.5507/fof.2017.024>, 2018.
554 Jung, P., Briegel-Williams, L., Schermer, M., and Büdel, B.: Strong in combination: Polyphasic approach
555 enhances arguments for cold-assigned cyanobacterial endemism, Microbiologyopen, 8, e00729,
556 <https://doi.org/10.1002/mbo3.729>, 2019.
557
558 Kampbell, D. H., Wilson, J. T., and Vandegrift, S. A.: Dissolved-oxygen and methane in water by a Gc
559 headspace equilibration technique, Int. J. Environ. Anal. Chem., 36, 249–257,
560 <https://doi.org/10.1080/03067318908026878>, 1989.
561 Kappler, A., Bryce, C., Mansor, M., Lueder, U., Byrne, J. M., and Swanner, E. D.: An evolving view on
562 biogeochemical cycling of iron, Nat. Rev. Microbiol., <https://doi.org/10.1038/s41579-020-00502-7>, 2021.
563
564 Kühnau, J.: Balneologisches Gutachten über die Heilwirkungen, welche von den im Stadtgebiet von Fürth
565 erbohrten Mineralquellen zu erwarten sind.- Unveröff. Gutachten, 14 S., 3 Tab., Wiesbaden, 1938.
566
567 Knox, M., Quay, P. D., and Wilbur, D.: Kinetic isotopic fractionation during air-water gas transfer of O₂, N₂;
568 CH₄, and H₂, J. Geophys. Res. Oceans, 97, 20335-20343, <https://doi.org/10.1029/92JC00949>, 1992.
569

hat formatiert: Deutsch (Deutschland)

hat formatiert: Deutsch (Deutschland)

hat formatiert: Deutsch (Deutschland)

Feldfunktion geändert

hat formatiert: Schriftart: (Standard) Times New Roman, 10 Pt., Deutsch (Deutschland)

hat formatiert: Schriftart: (Standard) Times New Roman, 10 Pt., Deutsch (Deutschland)

hat formatiert: Schriftart: (Standard) Times New Roman, 10 Pt., Englisch (Vereinigte Staaten)

hat formatiert: Schriftart: (Standard) Times New Roman, 10 Pt., Englisch (Vereinigte Staaten)

hat formatiert: Englisch (Vereinigte Staaten)

570 Köhler, I., Piatka, D., Barth, J. A. C., and Martinez, R. E.: Beware of effect on isotopes of dissolved oxygen
571 during storage of natural iron -rich water samples: A technical note, *Rapid Commun. Mass Spectrom.*, 35,
572 e9024, <https://doi.org/10.1002/rcm.9024>, 2020.

573

574 Komárek, J., and Anagnostidis, K.: Cyanoprokaryota. 2. Oscillatoriales, in: *Süßwasserflora von Mitteleuropa*,
575 edited by: Büdel, B., Krienitz, L., Gärtner, G., and Schagerl, M., Elsevier/Spektrum, Heidelberg, Germany, 759,
576 2005.

577

578 Kritzberg, E. S., and Ekström, S. M.: Increasing iron concentrations in surface waters- A factor behind
579 brownification?, *Biogeosciences Discuss.*, 8, 12285-12316, <https://doi.org/10.5194/bg-9-1465-2012>, 2011.

580

581 Kritzberg, E. S., Maher, Hasselquist, E., Skerlep, M., Löfgren, S., Olsson, O., Stadmark, J., Valinia, S., Hansson,
582 L. A., and Laudon, H.: Browning of freshwaters: Consequences to ecosystem services, underlying drivers, and
583 potential mitigation measures, *Ambio.*, 49, 375-390, <https://doi.org/10.1007/s13280-019-01227-5>, 2020.

584

585 Kroppnick, P. M.: Respiration, photosynthesis, and oxygen isotope fractionation in oceanic surface waters,
586 *Limnol. Oceanogr.*, 20, 988-992, <https://doi.org/10.4319/lo.1975.20.6.0988>, 1975.

587

588 Liger, E., Charlet, L., and Van Cappellen, P.: Surface Catalysis of Uranium(VI) Reduction by Iron(II), *Geochim.*
589 *Cosmochim. Acta.*, 63, 2939-2955, [https://doi.org/10.1016/S0016-7037\(99\)00265-3](https://doi.org/10.1016/S0016-7037(99)00265-3), 1999.

590

591 Llyod, R. M.: Oxygen isotope behavior in the Sulfate-Water System, *J. Geophys. Res.*, 73, 6099-6110,
592 <https://doi.org/10.1029/JB073i018p06099>, 1968.

593

594 Lu, J. -B. Jian, J., Huang, W., Lin, H., Li, J., and Zhou, M.: Experimental and theoretical identification of the
595 Fe(VII) oxidation state in FeO₄, *Phys. Chem. Chem. Phys.*, 18, 31125-31131,
596 <https://doi.org/10.1039/C6CP06753K>, 2016.

597

598 Mader, M., Schmidt, C., van Geldern, R., and Barth, J. A. C.: Dissolved oxygen in water and its stable isotope
599 effects: A review, *Chem. Geol.*, 473, 10-21, <https://doi.org/10.1016/j.chemgeo.2017.10.003>, 2017.

600

601 Mader, M., Roberts, A. M., Porst, D., Schmidt, C., Trauth, N., van Geldern, R., and Barth, J. A. C.: River
602 recharge versus O₂ supply from the unsaturated zone in shallow riparian groundwater: A case study from the
603 Selke River (Germany), *Sci Total Environ.*, 634, 374-381, <https://doi.org/10.1016/j.scitotenv.2018.03.230>, 2018.

604

605 Meurer, M., Banning, A.: Uranmobilisierung im Helgoländer Buntsandstein – Auswirkungen auf die Brack- und
606 Trinkwasserqualität. *Grundwasser*, 24, 43–50, <https://doi.org/10.1007/s00767-018-0408-1>, 2019.

607

608 Michaud, S. C., and Richardson, C. J.: Relative radial oxygen loss in five wetland plants, in: *Constructed Wetlands*
609 *for Wastewater Treatment*, edited by: Hammer, D. A., Lewis Publishers, Chelsea, USA, 501–507, 1989.

Feldfunktion geändert

hat formatiert: Schriftart: 10 Pt.

hat formatiert: Schriftart: 10 Pt.

hat formatiert: Schriftart: 10 Pt., Englisch (Vereinigte Staaten)

hat formatiert: Englisch (Vereinigte Staaten)

hat formatiert: Schriftart: 10 Pt., Englisch (Vereinigte Staaten)

hat formatiert: Englisch (Vereinigte Staaten)

hat formatiert: Schriftart: 10 Pt.

hat formatiert: Englisch (Vereinigte Staaten)

hat formatiert: Schriftart: 10 Pt., Englisch (Vereinigte Staaten)

hat formatiert: Englisch (Vereinigte Staaten)

610
611 Millero, F. J.: The effect of ionic interactions on the oxidation of metals in natural waters, *Geochim. Cosmochim.*
612 *Acta.*, 49, 547–53, [https://doi.org/10.1016/0016-7037\(85\)90046-8](https://doi.org/10.1016/0016-7037(85)90046-8), 1985.
613
614 Oba, Y., and Poulson, S. R.: Oxygen isotope fractionation of dissolved oxygen during reduction by ferrous iron,
615 *Geochim Cosmochim Acta.*, 73, 13-24, <https://doi.org/10.1016/j.gca.2008.10.012>, 2009.
616
617 Oba, Y, and Poulson, S. R.: Oxygen isotope fractionation of dissolved oxygen during abiological reduction by
618 aqueous sulfide, *Chem Geol.*, 268, 226-232, <https://doi.org/10.1016/j.chemgeo.2009.09.002>, 2009.
619
620 Park, B., and Dempsey, B. A.: Heterogeneous oxidation of Fe(II) on ferric oxide at neutral pH and a low partial
621 pressure of O₂, *Environ. Sci. Technol.*, 39, 6494–6500, <https://doi.org/10.1021/es0501058>, 2005.
622
623 Parker, S. R., Poulson, S. R., Gammons, C. H., and DeGrandpre, M. D.: Biogeochemical controls on diel cycling
624 of stable isotopes of dissolved oxygen and dissolved inorganic carbon in the Big Hole River, Montana, *Environ*
625 *Sci Technol.*, 39, 7134–7140, <https://doi.org/10.1021/es0505595>, 2005.
626
627 Parker, S. R., Gammons, C. H., Poulson, S. R., DeGrandpre, M. D., Weyer, C. L., Smith, M. G., Babcock, J. N.,
628 and Oba, Y.: Diel behavior of stable isotopes of dissolved oxygen and dissolved inorganic carbon in rivers over a
629 range of trophic conditions, and in a mesocosm experiment, *Chem Geol.*, 269, 22–32,
630 <https://doi.org/10.1016/j.chemgeo.2009.06.016>, 2010.
631
632 Parker, S. R., Gammons, C. H., Smith, M. G., and Poulson, S. R.: Behavior of stable isotopes of dissolved oxygen,
633 dissolved inorganic carbon and nitrate in groundwater at a former wood treatment facility containing hydrocarbon
634 contamination, *Appl. Geochem.*, 27, 1101-1110, <https://doi.org/10.1016/j.apgeochem.2012.02.035>, 2012.
635
636 Parker, S. R., Darvis, M. N., Poulson, S. R., Gammons, C. H., and Stanford, J. A.: Dissolved oxygen and dissolved
637 inorganic carbon stable isotope composition and concentration fluxes across several shallow floodplain aquifers
638 and in a diffusion experiment, *Biogeochemistry*, 117, 539-552, <https://doi.org/10.1007/s10533-013-9899-0>, 2014.
639
640 Parkhurst, D. L., and Appelo, C. A. J.: Description of input and examples for PHREEQC version 3—A computer
641 program for speciation, batch-reaction, one-dimensional transport, and inverse geochemical calculations. Volume
642 book 6 series Techniques and Methods. 2009.
643
644 Pati, S. G., Bolotin, J., Brennwald, M. S., Kohler, H. P. E., Werner, R. A., and Hofstetter, T. B.: Measurement of
645 oxygen isotope ratios (¹⁸O/¹⁶O) of aqueous O₂ in small samples by gas chromatography/isotope ratio mass
646 spectrometry, *Rapid Commun. Mass Spectrom.*, 30, 684–690, <https://doi.org/10.1002/rcm.7481>, 2016.
647
648 Pusch, M.: The metabolism of organic matter in the hyporheic zone of a mountain stream, and its spatial
649 distribution, *Hydrobiologia*, 323, 107-118, <https://doi.org/10.1007/BF00017588>, 1996.
650

Feldfunktion geändert

651 Quay, P. D., Wilbur, D. O., Richey, J. E., Devol, A. H., Benner, R., and Forsberg, B. R.: The ^{18}O : ^{16}O of
652 dissolved oxygen in rivers and lakes in the Amazon Basin: Determining the ratio of respiration to photosynthesis
653 rates in freshwater. *Limnol. Oceanogr.*, 40, 718-729, <https://doi.org/10.4319/lo.1995.40.4.0718>, 1995.
654
655 Schwertmann, U.: Solubility and dissolution of iron oxides, *Plant Soil*, 130, 1-25,
656 <https://doi.org/10.1007/BF00011851>, 1991.
657
658 Schwab, R. G.: Die natürliche Radioaktivität der Erdkruste, in: *Natürliche und künstliche Strahlung in der Umwelt.*
659 *Eine Bilanz vor und nach Tschernobyl*, edited by: Hosemann, G., and Wirth, E., Erlanger Forschungen Reihe B,
660 Erlangen, Germany, 25-43, 1987.
661
662 Sylvester, P., Westerhoff, P., Boyd, O., and Sengupta, A. K.: Arsen X^{np} - A new hybrid sorbent for arsenic removal
663 from drinking water, in: ACE '05, Proceedings of the AWWA Annual Conference and Exposition, San Francisco;
664 USA, 2005.
665
666 Skinner, B.J.: A Second Iron Age Ahead? *Res. J. Environ. Sci.*, 3, 559-575, <https://doi.org/10.1016/S0166->
667 [1116\(08\)71071-9](https://doi.org/10.1016/S0166-1116(08)71071-9), 1979.
668
669 Smith, L., Watzin, M. C., and Druschel, G.: Relating sediment phosphorus mobility to seasonal and diel redox
670 fluctuations at the sediment-water interface in a eutrophic freshwater lake. *Limnol. Oceanogr.*, 56, 2251-2264,
671 <https://doi.org/10.4319/lo.2011.56.6.2251>, 2011.
672
673 Stanier, R. Y., Kunisawa R., Mandel, M., and Cohen-Bazire, G.: Purification and properties of unicellular blue-
674 green algae (order Chroococcales). *Bacteriol. Rev.* 35, 171-205, <https://doi.org/10.1128/membr.35.2.171->
675 [205.1971](https://doi.org/10.1128/membr.35.2.171-205.1971), 1971.
676
677 Swanner, E. D., Mloszewska, A. M., Cirpka, O. A., Schoenberg, R., Konhauser, K. O., and Kappler, A.:
678 Modulation of oxygen production in Archaeal oceans by episodes of Fe(II) toxicity, *Nat. Geosci.*, 8,
679 <https://doi.org/10.1038/ngeo2327>, 126-130, 2015.
680
681 Taylor, B. E., and Wheeler, M. C.: Sulfur- and Oxygen-Isotope Geochemistry of Acid Mine Drainage in the
682 Western United States, in: *Environmental Geochemistry of Sulfide Oxidation* edited by: Alpers, C. N., and Blowes,
683 D. W., American Chemical Society Symposium Series, Washington DC, USA, 481-514, 1993.
684
685 Teal, J. M. and Kanwisher, J. W.: Gas Transport in the Marsh Grass, *Spartina alterniflora*, *J. Exp. Bot.*, 17, 355-
686 361, <https://doi.org/10.1093/jxb/17.2.355>, 1966.
687
688 van Geldern, R. and Barth, J. A. C.: Optimization of instrument setup and post-run corrections for oxygen and
689 hydrogen stable isotope measurements of water by isotope ratio infrared spectroscopy (IRIS), *Limnol.*
690 *Oceanogr. Methods*, 10, 1024-1036, <https://doi.org/10.4319/lom.2012.10.1024>, 2012.
691

692 Wand, X., and Veizer, J.: Respiration-photosynthesis balance of terrestrial aquatic ecosystems, Ottawa area,
693 Canada. *Geochim. Cosmochim. Acta.*, 64, 3775-3786, [https://doi.org/10.1016/S0016-7037\(00\)00477-4](https://doi.org/10.1016/S0016-7037(00)00477-4), 2000.
694
695 Wassenaar, L. I., and Koehler, G.: An on-line technique for the determination of the $\delta^{18}\text{O}$ and $\delta^{17}\text{O}$ of gaseous and
696 dissolved oxygen, *Anal. Chem.*, 71, 4965–4968, <https://doi.org/10.1021/ac9903961>, 1999.
697
698 Wassenaar, L. I., and Hendry, M. J.: Dynamics and stable isotope composition of gaseous and dissolved oxygen,
699 *Ground Water*, 45, 447–460, <https://doi.org/10.1111/j.1745-6584.2007.00328.x>, 2007.
700
701 Weyhenmeyer, G. A., Prairie, Y. T., and Tranvik, L. J.: Browning of Boreal Freshwaters Coupled to Carbon-
702 Iron Interactions along the Aquatic Continuum, *PLoS One*, 9, e88104,
703 <https://doi.org/10.1371/journal.pone.0088104>, 2014.
704
705 Wilmotte, A., Van der Auwera, G., and De Wachter, R.: Structure of the 16S ribosomal RNA of the thermophilic
706 cyanobacterium *Chlorogloeopsis* HTF (*Mastigocladus laminosus* HTF⁺) strain PCC75 18, and phylogenetic
707 analysis, *FEBS Lett.*, 317, 96–100, [https://doi.org/10.1016/0014-5793\(93\)81499-p](https://doi.org/10.1016/0014-5793(93)81499-p), 1993.
708
709 Zhang, Y., Charlet, L., and Schindler P. W.: Adsorption of protons, Fe(II) and Al(III) on lepidocrocite ($\gamma\text{-FeOOH}$),
710 *Colloids Surf.*, 63, 259-268, [https://doi.org/10.1016/0166-6622\(92\)80247-Y](https://doi.org/10.1016/0166-6622(92)80247-Y), 1992.
711
712